# Surface Modification and Characterization of Carbonized *Raphia taedigera* seed for the Adsorption of $Pb^{2+}$ from aqueous solution

**Nurudeen A. Abdulrahman[1], Akintayo Rotibi[2,] and Segun M. Abegunde[1]**

[1]Department of Science Technology, Federal Polytechnic, Ado-Ekiti, Nigeria
[2]Department of Minerals and Petroleum Resources Engineering Technology, Federal Polytechnic, Ado-Ekiti, Nigeria

DOI: 10.29322/IJSRP.10.09.2020.p10520
http://dx.doi.org/10.29322/IJSRP.10.09.2020.p10520

***Abstract***- *Raphia taedigera* activated carbon was prepared and impregnated with sodium dodecyl sulphate (SDS) and disodium ethylene diaminetetraacetic acid (EDTA) to enhance its performance for the adsorption of lead ions from aqueous solution. The two modified activated carbons, the sodium dodecyl sulphate modified *Raphia taedigera* activated carbon (SDS-RT) and the disodium ethylene diaminetetraacetic acid *Raphia taedigera* activated carbon (EDTA-RT), were characterized. Fourier transform infrared spectroscopy revealed the presence of C=C, OH, CN and CO at peaks 1584, 3753, 2000 and 1240 $cm^{-1}$, respectively, which all aid adsorption. Scanning electron microscopy coupled with Energy dispersive X-ray showed an aggregated surface morphology with pores and the carbon-oxygen ratio of 3.54 and 2.39 for SDS-RT and EDTA, respectively. The optimum performances of 97.70% and 94.25% were achieved for the adsorption of $Pb^{2+}$ onto SDS-RT and EDTA-RT, respectively; at pH 5 with 0.5 g using 25 mL of 100 mg/L lead ion solution. Material modified with SDS exhibited superior performances in all the adsorption conditions evaluated. Adsorption modelling showed the adsorption fit well into Langmuir isotherm model and follow the pseudo-second-order kinetic model. Thermodynamic studies showed that the adsorption processes are exothermic, feasible and spontaneous.

***Index Terms***- *Raphia taedigera;* Activated carbon; Adsorption; Lead.

## I. INTRODUCTION

Heavy metal pollution is one of the prominent environmental issues of the present century. Due to the advancement in industrial activities such as smelting, metal plating, mining, paint, and metallurgical industries, more heavy metal pollutants are released into the environment [1]. Heavy metals such as lead, chromium, mercury, arsenic, nickel and copper find their ways into the water bodies through the indiscriminate discharge of industrial and agricultural waste. Heavy metal contamination can also occur through atmospheric deposition, metal corrosion, soil erosion and leaching of heavy metals, sediment re-suspension and metal evaporation from water resources to soil and groundwater [2, 3]. The presence and accumulation of heavy metals in aquatic environments pose a significant threat to man, animal and plant [4].

Among the commonly encountered metal pollutants, lead is one of the most dangerous water pollutants. Lead toxicity has been a subject of interest for environmental researchers because of its toxic effect on plants, animals, and humans [5, 6]. Various industrial activities such as the extraction and processing of solid minerals, metal plating, oil refining, and battery manufacturing among others, had been recognized as the primary means of releasing lead into the environment [7]. Both Standard Organization of Nigeria and National Agency for Food and Drug Administration and Control set the maximum permissible limit of Pb in drinking water at 0.01 mg/L [8]. At higher concentration, serious health problems can occur. Lead toxicity poisoning in the human body can be devastating. Lead poisoning can cause anaemia, kidney damage, and toxicity symptoms including, impaired kidney function, headache and hypertension [9, 10]. Lead is highly persistent in the environment, and because of its continuous use, its levels rise in almost every country, posing serious threats. Several methods, including Fenton process, degradation by photocatalytic processes, chemical coagulation/flocculation, ozonation, oxidation, chemical precipitation, adsorption, ion exchange and reverse osmosis [11 – 14] had been used. Adsorption, among others, has proved to be an effective, cheap, simple and save technique for wastewater treatment [15]. Adsorption techniques use porous materials with large surface area and suitable surface chemistry. Materials such as clay, silica gel, activated carbon, synthetic resins, molecular sieve zeolites, impregnated biomaterials and nanoparticles have been extensively used as adsorbents for industrial applications in water and wastewater purifications [14]. Recently, agricultural waste products have found applications as biosorbents for adsorption process. Thus, this present work aims at using sodium dodecyl sulphate ($C_{12}H_{25}O_4S.Na$), and disodium ethylenediaminetetraacetic acid ($C_{10}H_{16}N_2Na_2O_8$) modified activated carbons prepared from *Raphia taedigera* seed for the removal of Pb ions from aqueous solution.

## II. MATERIALS AND METHODS

Sample preparation

*Raphia taedigera* seeds were obtained from Ado-Ekiti. The seeds were washed under running water, sun-dried and crushed. The crushed sample was kept in an airtight plastic container for further analysis.

Preparation of *Raphia taedigera* adsorbent

Carbonization

The carbonization of *R. taedigera* was done using method reported by Bello *et al.*, [16] and Olasehinde and Abegunde [15]. The crushed *R. taedigera* seeds were carbonized by placing 100 g of the seed in a muffle furnace at 350 ° C for 2 hours.

Chemical activation of the carbonized material

The chemical activation was done on the carbonized material. 20 g of carbonized material was weighed and transferred into a clean 500 mL beaker containing 200 mL 0.1 M sodium dodecyl sulphate, homogenized and left to stand for 24 hours. The impregnated materials were filtered and the residue was rinsed with 200 mL distilled water to attain a pH of 7. The acid-free residue was dried to a constant weight at 105 ° C for 4 hours [17]. The dried activated carbon was sieved with 100-mm mesh to obtain a fine powder of *Raphia taedigera* activated carbon labelled as SDS-RT. The procedure was repeated using disodium ethylenediaminetetraacetic acid as activating agent and the product labelled as EDTA-RT. The activated carbons were stored in a separate airtight container for further use.

Preparation of Pb (II) Solution

1000 mg/L of lead nitrate stock solution was prepared by dissolving 1.6 g $Pb(NO_3)_2$ in distilled water in 1000 mL volumetric flask and made up to the mark with distilled water. 0.1 M HCl and 0.1 M NaOH solutions were also prepared to adjust the solution pH. All reagents used were of pure analytical grade.

Batch Adsorption Studies and the Evaluation of Adsorption Condition

Batch adsorption studies were carried out by shaking 0.50 g of activated carbons (SDS-RT and EDTA-RT) separately with 25 mL of 100 mg/L Pb (II) solution in a 125 mL Erlenmeyer flask. The pH of the solution was adjusted using 0.1 M HCl or 0.1 M NaOH solution to 7. The flask was agitated at 120-rpm for 60 min to ensure equilibrium was reached. The solution was filtered with Whatman No 42 filter paper and the filtrate stored in the sample bottle. AAS was used to determine the concentration of $Pb^{2+}$ in the filtrate. The quantity adsorbed by the ACs was determined using Equation 1. The efficiency of the adsorbent was determined using Equation 2. The effects of adsorption conditions such as contact time, solution pH, temperature, adsorbate concentration and adsorbent dosage were determined. This was done at constant conditions except the condition under examination. The quantity adsorbed and efficiency of the adsorbent were evaluated using Equations 1 and 2 respectively.

$$q_e = \frac{(C_o - C_e)V}{W} \quad (1)$$

$$\text{Adsorption efficiency} = \frac{(C_o - C_e)}{C_o} \text{ x } 100 \quad (2)$$

Where, $q_e$ is the quantity of $Pb^{2+}$ adsorbed per unit mass in mg/g, $C_o$ is the initial $Pb^{2+}$ concentration in mg/L, $C_e$ is the $Pb^{2+}$ concentration at equilibrium in mg/L, $V$ is the volume of $Pb^{2+}$ solution in millilitres and $W$ is the mass of the adsorbent in grams.

Material Characterisation

The functional groups in the activated carbon were determined using Agilent Cary 630 FTIR instrument with scanning range 4000 – 650 $cm^{-1}$. The surface morphology examination of the prepared materials was carried out by Phenom ProX SEM at HV value of 15 KV coupled with EDX.

Adsorption Isotherm

Isotherm predicts the relationship between adsorbent and adsorbate [18]. It explains how adsorbent materials interact with pollutants. The results of this present work are modelled by Langmuir and Freundlich isotherm models.

Langmuir Isotherm

Langmuir isotherm is based on the assumption that maximum adsorption corresponds to a saturated monolayer of solute molecules on the adsorbent surface, that the energy of adsorption is constant, and that there is no transmigration of adsorbate in the plane of the surface [19].

Langmuir isotherm model can be expressed as;

$$q_e = \frac{q_{max} b C_e}{1 + K_L C_e} \quad (3)$$

The linear expression of this isotherm can be written as Equation 4

$$\frac{C_e}{q_e} = \frac{1}{K_L q_m} + \frac{C_e}{q_m} \quad (4)$$

Where $q_e$ and $q_{max}$ are the equilibrium and the maximum amount of the metal per unit weight of the adsorbent respectively, $C_e$ is the residual metal concentration at equilibrium (mg/L), and $K_L$ is a constant related to the affinity of the binding sites.

The shape of this isotherm can also be expressed in terms of separation factor ($R_L$) [20], which is given as follows:

$$R_L = \frac{1}{1 + KLCo} \quad (5)$$

Where $K_L$ (L/mg) is Langmuir constant and $C_o$ is the initial MB concentration in mg/L.

Freundlich isotherm

The Freundlich isotherm assumes adsorption takes place on a heterogeneous surface with a non-uniform distribution of heat of biosorption through a multilayer adsorption mechanism [17]. It is expressed by Equation 6.

$$q_e = K_f C_e^{1/n} \quad (6)$$

The logarithmic form of the Equation becomes:

$$\log q_e = \log K_f + \frac{1}{n}\log C_e \quad (7)$$

Where $q_e$ is the equilibrium amount adsorbed (mg/g), $C_e$ the equilibrium concentration of the adsorbate (mg/L), $K_f$ and $n$ are Freundlich constants.

Kinetic Isotherm

The adsorption kinetics in wastewater treatment is significant as it provides valuable insights into the reaction pathways and the mechanism of an adsorption reaction [15]. Pseudo-first-order and pseudo-second-order kinetic models are used for the present work.

Pseudo-first-order kinetic model

Pseudo - first-order kinetic model assumes that the overall adsorption rate is directly proportional to the driving force, that is, the difference between initial and equilibrium concentration of the adsorbate, $(q_{eq} - q_t)$ [21]. Therefore, the pseudo-first-order kinetic can be expressed in linearized form as Equation 7.

$$\log(q_{eq} - q_t) = log(q_{eq} - \frac{k_1 t}{2.303}) \quad (8)$$

Where $q_{eq}$ is the amount of $Pb^{2+}$ adsorbed at equilibrium (mg/g), $q_t$ is the amount of $Pb^{2+}$ adsorbed at time t (mg/g); $k_1$ is the equilibrium rate constant of pseudo-first sorption ($min^{-1}$).

A straight line plot of log ($q_e$ -$q_t$) versus $t$ suggest the applicability of this kinetic model.

Pseudo-second-order kinetic model

The pseudo-second-order reaction kinetics model is based on the sorption equilibrium capacity. The linearized form can be expressed as:

$$\frac{t}{q_t} = \frac{1}{k_2 q_e^2} + \frac{1}{q_e} \quad t \quad (9)$$

Where, $q_t$ is the amount of $Pb^{2+}$ adsorbed at time t (mg/g); $k_2$ is the equilibrium rate constant for the pseudo-second- order adsorption (g/mg/min).

A plot of $t/q_t$ versus $t$ should give a straight line of pseudo-second-order kinetics where $q_e$ and $k_2$ can be determined from the slope and intercept of the plot, respectively.

Thermodynamic Studies

The values of the thermodynamic parameters such as a change in free energy ($\Delta G^0$), enthalpy ($\Delta H^0$) and entropy ($\Delta S^o$) help to have a better understanding of the temperature effect on the adsorption [17, 21]. The thermodynamic parameters can be evaluated using Equation 10:

$$K_c = \frac{Cs}{Ce} \quad (10)$$

Where $C_s$ is the metal ions concentration on the ACs at equilibrium in mg/g, $C_e$ is the equilibrium concentration of the metal ions in a solution in mg/L, and $K_c$ is the thermodynamic equilibrium constant.

The Gibbs free energy, $\Delta G^o$ (kJ/mol) for the adsorption metal onto the adsorbents can be calculated using Equation 11:

$$\Delta G^o = -RT ln\, K_c \quad (11)$$

Enthalpy and entropy are obtained using Van't Hoff's Equation [21]:

$$\Delta G^0 = \Delta H^0 - T\Delta S^0 \quad (12)$$

$$\ln Kc = \frac{\Delta S^0}{R} - \frac{\Delta H^0}{RT} \quad (13)$$

Where $T$ is the absolute temperature (K), $R$ is the universal gas constant (8.314 J/mol/k), $\Delta H^o$ is changed in enthalpy, and $\Delta S^o$ is the degree of disorderliness of a reaction.

## III. Result and Discussion

FTIR Spectral analysis

FTIR analysis was done to know the functional groups in activated carbons. The spectral for SDS-RT and EDTA-RT were presented in Figures 1 and 2, respectively. The spectral revealed the presence of a band at about 3753 $cm^{-1}$ corresponding to free OH group, a band at about 2000 $cm^{-1}$corresponding to stretching vibration of -C≡N, a band at 1584 $cm^{-1}$ corresponding to stretching vibration of aromatic C=C, a band at 1240 $cm^{-1}$ corresponding to stretching vibration of carboxyl group C=O. However, Figure 1 revealed the presence of a band at about 2877 $cm^{-1}$ corresponding to Aliphatic C-H group, a band at about 1423 cm-1corresponding to =C-H bending vibration alkane which were not present in Figure 2. The difference in the FTIR spectral of the materials may be due to the different chemical used for surface modifications during the production process [22]. A similar result was reported by Olasehinde and Abegunde [15].

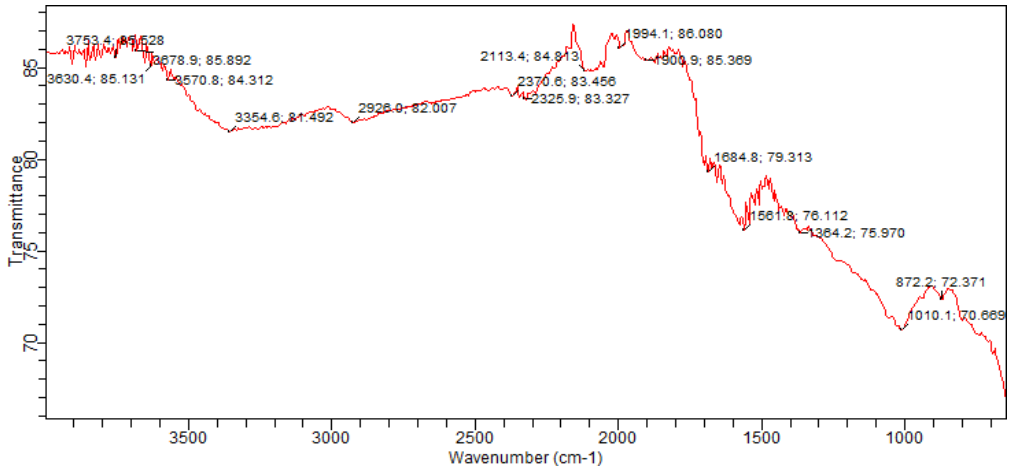


**Figure 1: FTIR Spectrum of SDS-RT**

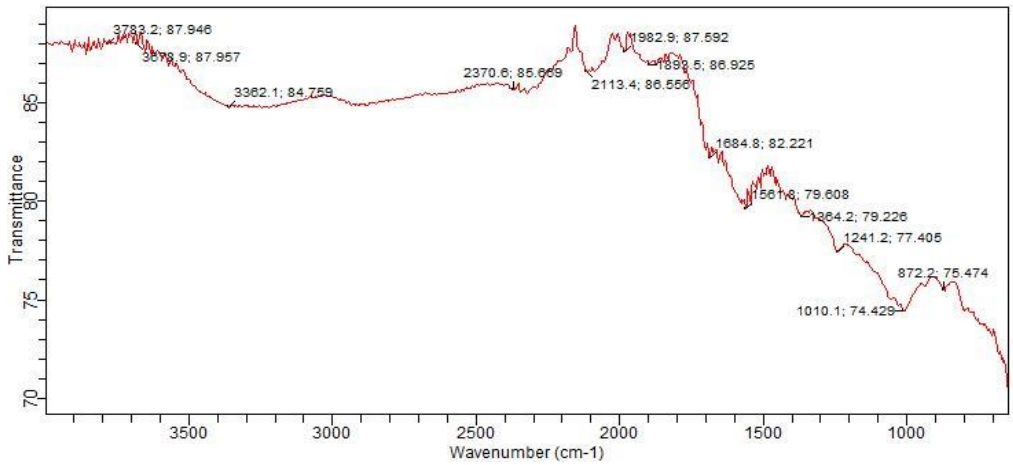


**Figure 2: FTIR Spectrum of EDTA-RT**

SEM Result

The surface morphologies of the SDS-RT and EDTA-RT were observed using scanning electron microscope. The micrographs at magnification 500x are presented in Figures 3 and 4. The SEM revealed an aggregated and rough surface morphology with pores at the surfaces of the ACs. Semi-quantitative chemical elemental analysis was conducted using EDX coupled with SEM. The detector allows the detection of elements such as C and O. EDX results of SDS-RT and EDTA-RT presented in Figures 3 and 4. The figures revealed the ratio of carbon to oxygen (C/O) in the two samples as 3.54 and 2.39 for SDS-RT and EDTA-RT, respectively. The high ratio of carbon to oxygen can be due to pyrolysis and chemicals used for surface modification. Sample rich in carbon content is a good and effective adsorbent for the removal of heavy metals, dyes and other organic pollutants from an aqueous solution [23]. This result was in agreement with previous reports by Bello *et al*., [16].

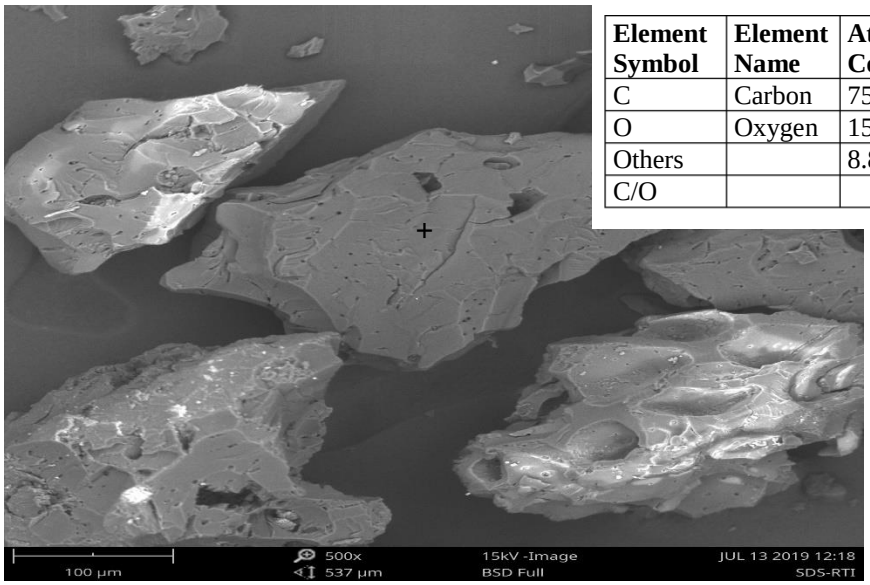


| Element Symbol | Element Name | Atomic Conc. | Weight Conc. |
|---|---|---|---|
| C | Carbon | 75.25 | 71.09 |
| O | Oxygen | 15.95 | 20.07 |
| Others | | 8.80 | 8.84 |
| C/O | | | 3.54 |

**Figure 3:** SEM image of SDS-RT with EDX

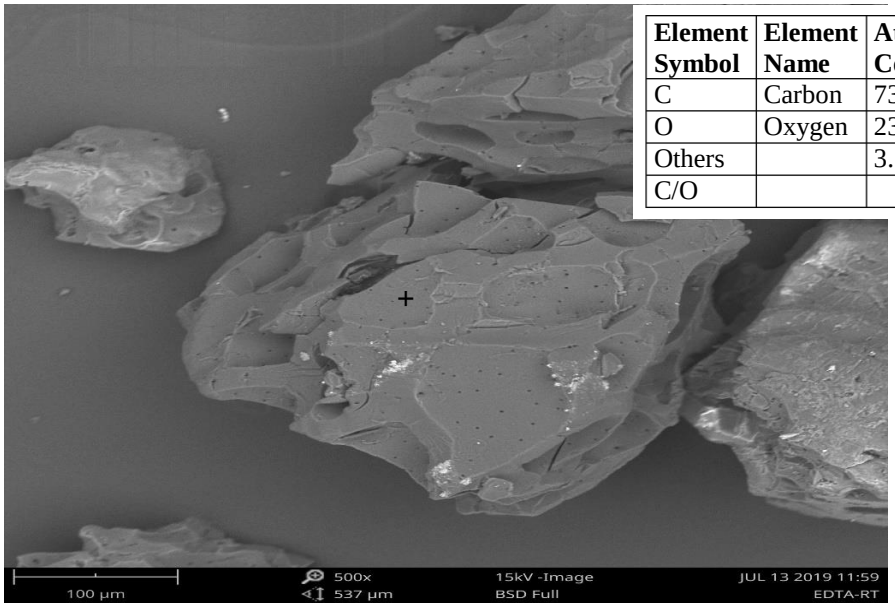


| Element Symbol | Element Name | Atomic Conc. | Weight Conc. |
|---|---|---|---|
| C | Carbon | 73.73 | 66.81 |
| O | Oxygen | 23.11 | 27.90 |
| Others | | 3.16 | 5.29 |
| C/O | | | 2.39 |

**Figure 4:** SEM image of EDTA-RT with EDX

Effect of Parameters in Adsorption Experiments

Effect of Contact Time

Equilibrium time is used to evaluate the efficiency and feasibility of an adsorbent. The adsorbent-adsorbate equilibrium time was evaluation at the time range of 10, 30, 60, 90 and 120 min using 100 mg/L $Pb^{2+}$ on 0.5 g adsorbent, agitated at 120-rpm at room temperature. The plot of efficiency percentage against time is presented in Figure 5. From the plots, it was observed that the efficiencies of SDS-RT and EDTA-RT increased with increasing contact time. The highest performance of 98.663 and 97.001% obtained for SDS-RT and EDTA-RT respectively at 120 min. The rapid adsorption at the initial stage could be as a result of the availability of abundant vacant sites on the surfaces of the adsorbents [22]. The responses of the adsorbents to time were in accordance with previous reports by AbdulRahman *et al.*, [10, 24]

Effect of pH

The pH of an aqueous solution is an important controlling factor that influences the uptake of the adsorbate. The pH influences the surface charge of the adsorbent particle and the degree of the ionization and speciation of the adsorbate. The effect of pH on the adsorption was experimented using 0.5 g AC, in 60 min with 25 mL of 100 mg/L $Pb^{2+}$ agitated at 120-rpm. The pH of the solution was adjusted using 0.1 M sulphuric acid or 0.1

M sodium hydroxide. The plots of percentage of $Pb^{2+}$ removal by SDS-RT and EDTA-RT against pH are presented in Figure 6. From the plots, the percentage removal increased with increasing pH until the pH maximum removal was attained at pH 5.for both SDS-RT and EDTA-RT. Low adsorption of $Pb^{2+}$ at low pH is probably due to the presence of $H^+$ ions competing with the metal ions for the adsorption sites. This result supports that the adsorption depends significantly on the pH of the surrounding solution, which affects the adsorbent surface charge and the degree of ionization of the adsorbate [25].

Effect of Temperature

The temperature dependence of adsorption capacity of SDS-RT and EDTA-RT for the adsorption of $Pb^{2+}$was investigated. The evaluation was done at 298, 303, 308, 313 and 318 K on 0.5 g with 25 mL of 100 mg/L $Pb^{2+}$ agitated at 120-rpm for 60 min. The plots of the adsorbent efficiency against temperature are presented in Figure 7. An increase in the percentage removal was observed up to 313 K for both ACs. The results showed the adsorption system could be exothermic which indicates that an increase in the temperature will result to an increase in desorption of the adsorbed $Pb^{2+}$. Similar result was reported by Sari *et al.*, [26].

Effect of Initial Concentration of Solution

The adsorbate concentration provides the needed driving force to overcome mass transfer resistance of the adsorbate between aqueous and solid phase. The effect of initial concentrations was determined with the initial $Pb^{2+}$concentrations of 20, 40, 60, 80 and 100 mg/L onto 0.5 g AC agitated for 60 min. Figure 8 presented the responses of SDS-RT and EDTA-RT for the adsorption of $Pb^{2+}$. The percentage removal increased with increasing in initial concentration for two ACs. The observed percentage removal increase can be attributed to the driving force due to a higher initial concentration of the solution. This was in agreement with earlier reports that pollutant removal through the adsorption process is concentration-dependent [27].

Effect of Adsorbent Dosage

Adsorbent dosage is crucial to adsorption process because it provides the binding sites for the uptake of the pollutant from solution. The adsorbent surface chemistry determines the potential of the adsorbent to remove metal pollutants. The dosage effect of the ACs was evaluated for the removal of $Pb^{2+}$ from aqueous solution using 0.1, 0.3, 0.5, 0.7 and 0.9 g of the ACs, 25 mL of 100 mg/L $Pb^{2+}$, at room temperature for 60 minutes. The plot of the percentage of removal against the ACs dosage was presented in Figure 9. The plot showed an increased in percentage removal with increase in the ACs dosage. The increase observed in the percentage removal by the two ACs could be due to the increase in the number of active sites at the surface because of the increase in the bulk of the adsorbents [25].

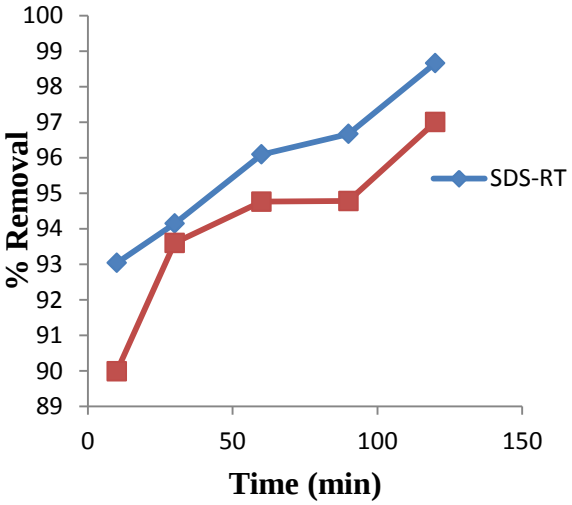


**Figure 5: Effect of contact time**

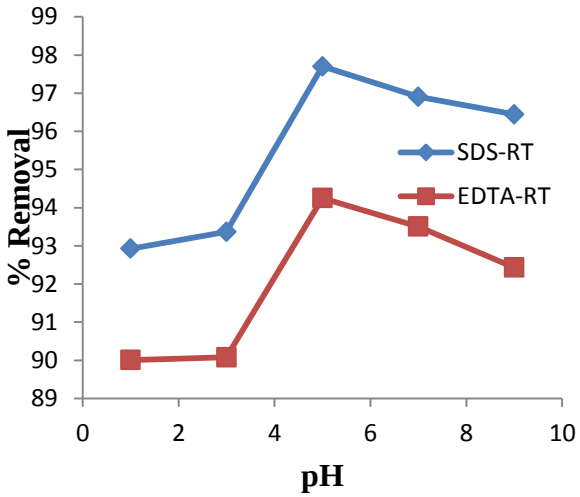


**Figure 6: Effect of solution pH**

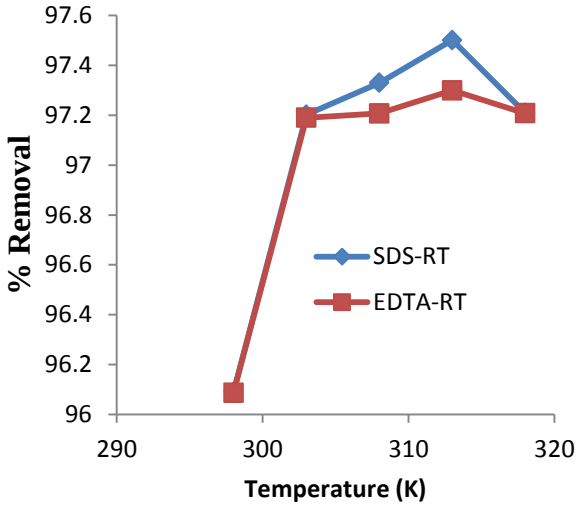


**Figure 7: Effect of Temperature**

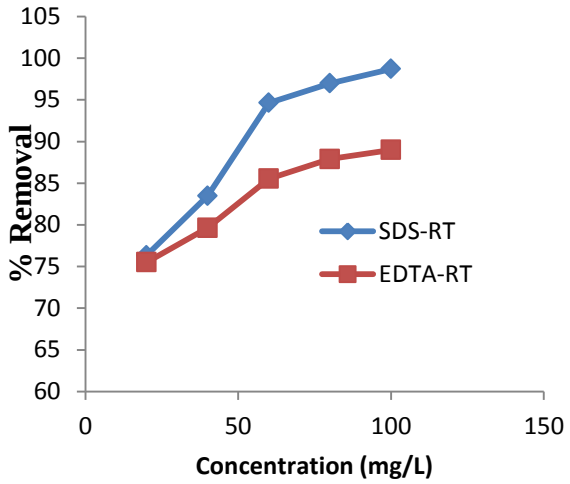


**Figure 8: Effect of initial concentration**

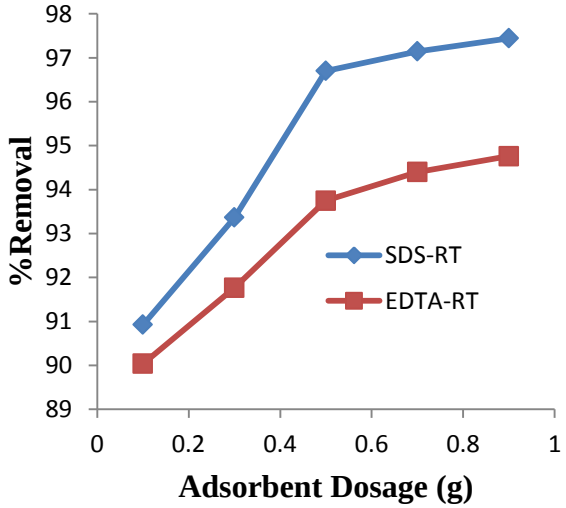


**Figure 9: Effect of Adsorbent Dosage**

Adsorption Isotherm

Adsorption isotherm explains the interaction between adsorbent and pollutants; hence, it is, necessary to establish the most suitable correlation for the equilibrium curve. The adsorption isotherm models employed in this study are Langmuir and Freundlich adsorption isotherm models. Langmuir isotherm plots of $C_e/q_e$ against $C_e$ for the adsorption of $Pb^{2+}$ onto SDS-RT and EDTA-RT at temperature values of 298, 308 and 318 K are presented in Figures 10 and 11, respectively. From the plots, the correlation coefficients ($R^2$) values equal to 1 for both ACs at all temperatures indicating a perfect relationship between the adsorption data. The values of $q_{max}$ obtained from the Langmuir plots and the calculated $q_e$ are presented in Table 1. The value of $q_{max}$ was very close to its corresponding calculated value, $q_e$ indicating Langmuir isotherm gives a good fit for the adsorption of $Pb^{2+}$ onto the adsorbents. Separation factor ($R_L$) was evaluated using Equation 5 to establish if the adsorption process is favourable or not. The $R_L$ value determines the shape of the isotherm to be unfavourable ($R_L > 1$), linear ($R_L = 1$), favourable ($0 < R_L < 1$), or irreversible ($R_L = 0$). The values of separation factor ($R_L$) at all temperatures were greater than 0 and less than 1 for both ACs, indicating favourable adsorptions.

The Freundlich isotherm describes heterogeneous adsorption process. It assumes adsorption takes place on a heterogeneous surface with a non-uniform distribution of heat of biosorption through a multilayer adsorption mechanism (Rauf, 2008). Plots of log $q_e$ against log $C_e$ representing Freundlich isotherm are presented in Figures 12 and 13 for SDS-RT and EDTA-RT respectively. The correlation coefficients ($R^2$) from the plots are contained in Table 1. The correlation coefficients

($R^2$) at all temperatures are > 0.97, indicating a strong relationship between the adsorption data. The values of *1/n* below 1 indicate a normal Langmuir isotherm. The results of the adsorption isotherm model suggest Langmuir isotherm with a better conformation for the adsorption of $Pb^{2+}$ onto SDS-RT and EDTA-RT.

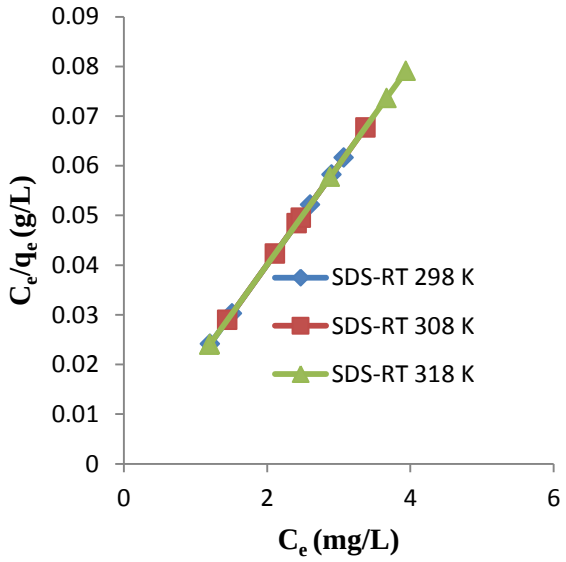


**Figure 10: Langmuir isotherm plot for the adsorption of $Pb^{2+}$ on SDS-RT**

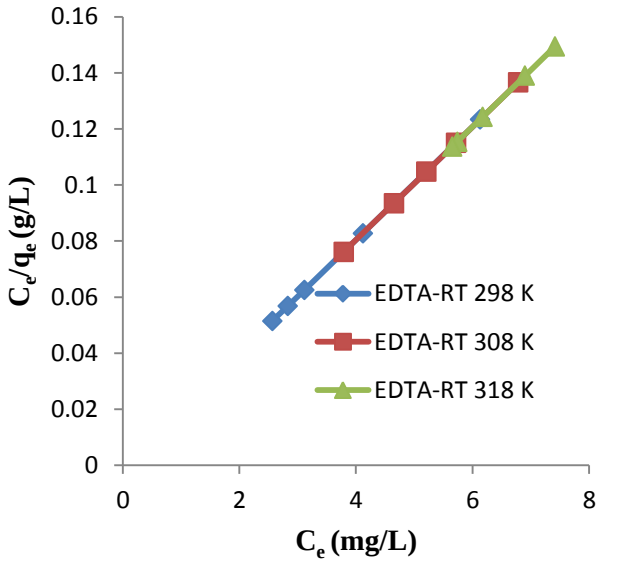


**Figure 11: Langmuir isotherm plot for the adsorption of $Pb^{2+}$ on EDTA-RT**

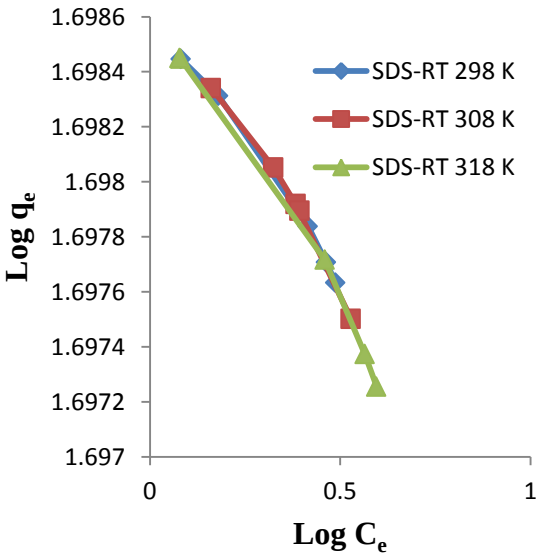


**Figure 12: Freundlich isotherm plot for the adsorption of $Pb^{2+}$ on SDS-RT**

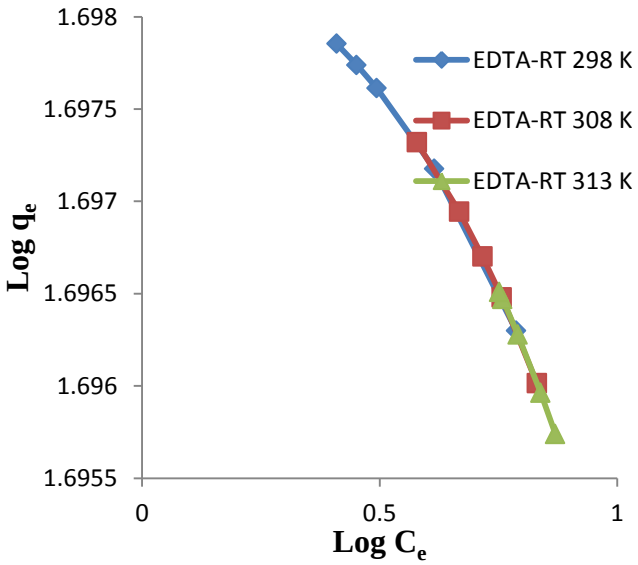


**Figure 13: Freundlich isotherm plot for the adsorption of $Pb^{2+}$ on EDTA-RT**

**Table 1: Results of adsorption isotherm for the adsorption of $Pb^{2+}$ onto SDS-RT and EDTA-RT**

| Isotherms Equation | Parameters | SDS-RT | | | EDTA-RT | | |
|---|---|---|---|---|---|---|---|
| | | 298 K | 308 K | 318 K | 298 | 308 K | 318 K |
| Langmuir $\frac{Ce}{qe} = \frac{1}{KLqm} + \frac{Ce}{qm}$ | Exp. $q_m$ | 49.75 | 49.75 | 49.75 | 49.51 | 49.51 | 49.26 |
| | Cal. $q_e$ (mg/g) | 49.87 | 49.81 | 49.72 | 49.87 | 49.81 | 49.72 |
| | $K_L$ (L/mg) | 251.26 | 201.01 | 201.01 | 67.34 | 40.40 | 25.38 |
| | $R_L$ x $10^{-3}$ | 0.04 | 0.05 | 0.05 | 0.15 | 0.25 | 0.39 |
| | $R^2$ | 1.00 | 1.00 | 1.00 | 1.00 | 1.00 | 1.00 |
| Freundlich $log\ qe = log\ Kf + \frac{1}{n} log\ Ce$ | -1/n x $10^{-2}$ | 0.20 | 0.22 | 0.22 | 0.41 | 0.51 | 0.65 |
| | -N x $10^2$ | 5.00 | 4.55 | 4.55 | 2.44 | 1.96 | 1.54 |
| | $K_f$ | 49.96 | 49.97 | 49.96 | 50.07 | 50.15 | 50.28 |
| | $R^2$ | 0.99 | 0.98 | 0.99 | 0.99 | 0.99 | 0.99 |

Adsorption Kinetics

Pseudo-first-order and the pseudo-second-order kinetic models were used to model the adsorption data in order to investigate the mechanism of adsorption of $Pb^{2+}$ onto SDS-RT and EDTA-RT. These empirical mathematical models are proven useful as tools for scale-up process optimization [15]. A plot of *Log* $(q_{eq} - q_t)$ against *t* representing Pseudo-first-order kinetic model are presented in Figures 14 and 15. The values of the $q_e$, $k_1$ and $R^2$ obtained from the plots are presented in Table 2. The value of $R^2$ at all temperatures was greater than 0.7 but less than 1, indicating a strong relationship between the data. However, the calculated value of $q_e$ was far below the corresponding experimental values; hence; the pseudo-first-order kinetic model cannot be said to be the best fit for the present work.

The Pseudo-second-order linearized Equation is expressed as given in Equation 9. The plots of *t/qt* against *t* for the kinetic model are presented in Figure 16. The pseudo-second-order parameters $q_e$, $k_2$ and $R^2$ were calculated for the two adsorbents and presented in Table 2. The value of $R^2$ was found to be 1.000 at each temperature for both SDS-RT and EDTA-RT, indicating a perfect relationship between the adsorption data. Also, from Table 2, the value of $q_{e(cal)}$ was close to the corresponding $q_{e(exp)}$ value for the adsorption $Pb^{2+}$ onto the two ACs.

The results of the kinetic modelling showed that the pseudo-second-order kinetic model has a better agreement with the adsorption data. The applicability of the pseudo-second-order model predicts that chemical reaction might be responsible for adsorption of $Pb^{2+}$ onto SDS-RT and EDTA-RT. The results of similar findings have been reported for the adsorption of $Pb^{2+}$onto Onion skin [21].

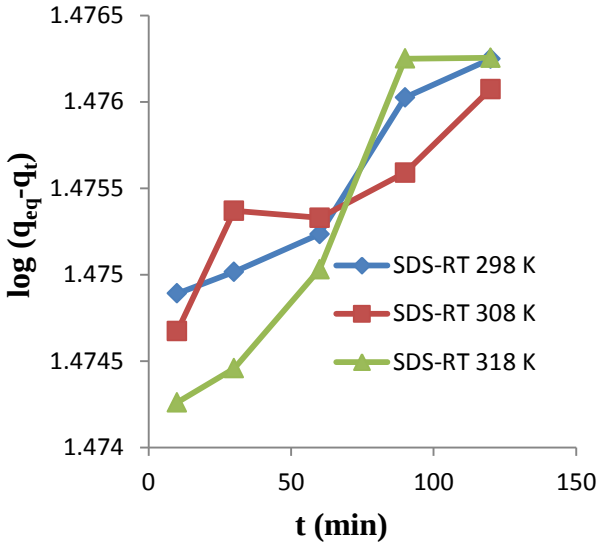


**Figure 14: Plot of Pseudo-first-order Kinetic model for the adsorption of $Pb^{2+}$ on SDS-RT**

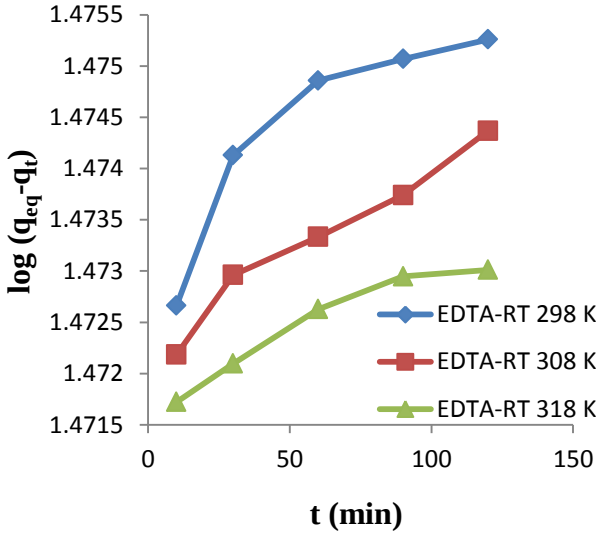


**Figure 15: Plot of Pseudo-first-order Kinetic model for the adsorption of $Pb^{2+}$ on EDTA-RT**

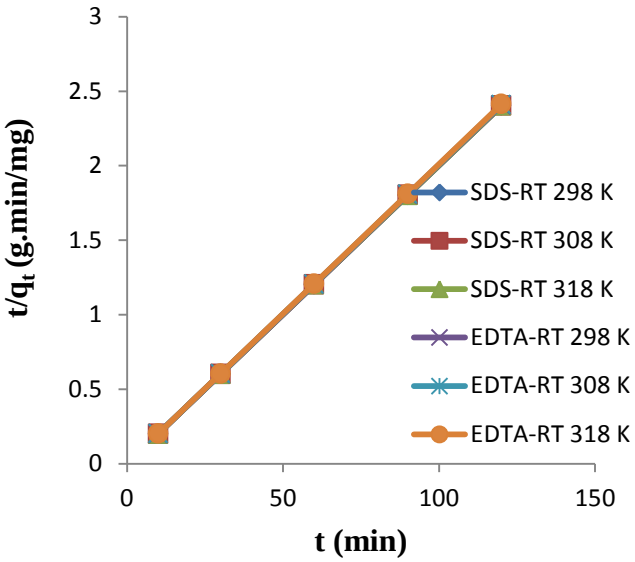


**Figure 16: Plot of Pseudo-second-order Kinetic model for the adsorption of $Pb^{2+}$ on SDS-RT and EDTA-RT**

**Table 2: Results of Adsorption Kinetics Parameters of the adsorption**

| Kinetic Model | Parameters | SDS-RT | | | EDTA-RT | | |
|---|---|---|---|---|---|---|---|
| | | 298 K | 308 K | 318 K | 298 K | 308 K | 318 K |
| **Pseudo-first-order** $\frac{1}{qt}=\frac{K1}{qet}+\frac{1}{qe}$ | $q_e$ *(mg/g)* | 29.83 | 29.84 | 29.79 | 29.72 | 29.66 | 29.63 |
| | $K_1$ x $10^{-3}$ | 0.02 | 0.02 | 0.05 | 0.05 | 0.05 | 0.02 |
| | $R^2$ | 0.94 | 0.86 | 0.93 | 0.79 | 0.96 | 0.93 |
| **Pseudo- second-order** $\frac{t}{qt}=\frac{1}{K2q2e}+\frac{1}{qe}t$ | $q_e$ *(mg/g)* | 50.00 | 50.00 | 50.00 | 50.00 | 49.75 | 49.75 |
| | $K_2$*(g/mg/min)* | 0.40 | 0.57 | 0.29 | 0.40 | 0.34 | 0.58 |
| | $R^2$ | 1.00 | 1.00 | 1.00 | 1.00 | 1.00 | 1.00 |

Thermodynamic Studies

The values of thermodynamic parameters such as Gibbs free energy change (*ΔG*), enthalpy change (*ΔH*) and entropy change (*ΔS*) are the real indicators for practical application of the adsorption technique. A plot of *ln* $K_c$ against *1/T* for the adsorption of $Pb^{2+}$ onto SDS-RT and EDTA-RT is presented in Figure 17. The thermodynamic were determined and presented in Table 3. From Table 3, the values of *ΔG* and *ΔH* are negative, while the value of *ΔS* is positive.. The negative values of the *ΔG* indicate spontaneous and feasible adsorption process. The negative value of $\Delta H^{o}$ confirmed that the adsorption of $Pb^{2+}$ onto SDS-RT and EDTA-RT were exothermic. The positive value of entropy indicates that the degrees of disorderliness increased at the AC-metal ion interface during the adsorption process predicting a low energy of attraction between the adsorbent and metal ions [15].

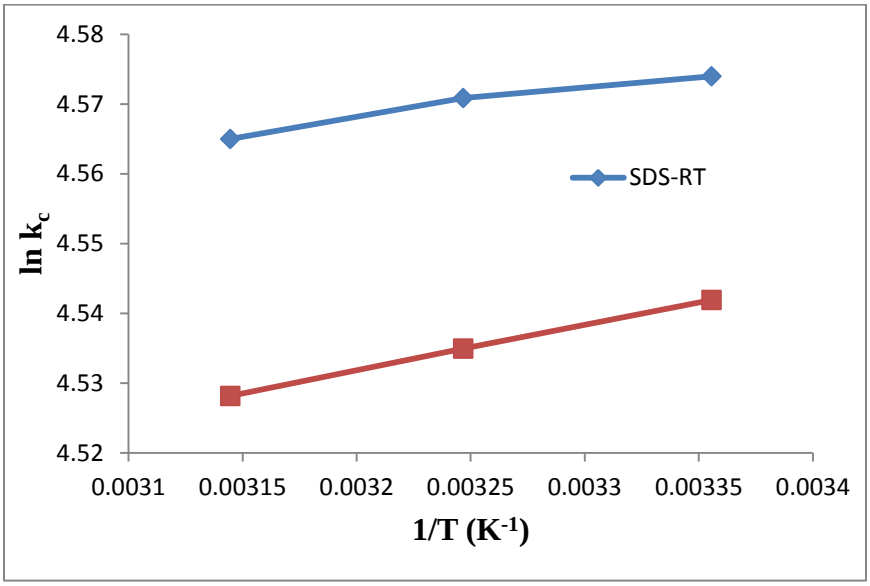


**Figure 17: Thermodynamic parameters for the adsorption of $Pb^{2+}$ on SDS-RT and EDTA-RT**

**Table 3: Thermodynamic parameters for the adsorption of $Pb^{2+}$ on SDS-RT and EDTA-RT**

| Adsorbent | Temperature | $\Delta G^0$ (KJ/mol) | $\Delta H^0$ (KJ/mol) | $\Delta S^0$(J/mol/K) |
|---|---|---|---|---|
| SDS-RT | 298 K | -11.33 | | |
| | 308 K | -11.70 | -0.35 | 36.85 |
| | 318 K | -12.07 | | |
| EDTA-RT | 298 K | -11.25 | | |
| | 308 K | -11.61 | -0.54 | 35.94 |
| | 318 K | -11.97 | | |

## IV. CONCLUSION

Sodium dodecyl sulphate (SDS) and disodium ethylene diaminetetraacetic acid (EDTA) modified activated carbons were successfully prepared from *Raphia taedigera* seed. The two activated carbons showed the presence of some functional groups that are important for the adsorption of metal ions from aqueous solution. The carbon-oxygen ratio of 3.54 and 2.39 for SDS-RT and EDTA, respectively were calculated indicating the potentiality of material for adsorption process. The optimum performance of 97.70% was obtained for the adsorption of $Pb^{2+}$ onto SDS-RT while the optimum performance of 94.25% was achieved for the adsorption of $Pb^{2+}$ onto EDTA-RT at pH 5 with 0.5 g using 25 mL of 100 mg/L lead ion solution. Adsorption modelling showed the adsorption processes best fit into Langmuir isotherm model and follow the pseudo-second-order kinetic model. Thermodynamic studies showed that the adsorption processes are exothermic, feasible and spontaneous. The results of the present work showed that the sodium dodecyl sulphate (SDS) and disodium ethylene diaminetetraacetic acid (EDTA) modified activated carbons prepared from *Raphia taedigera* seed are good adsorbents for the removal of lead ions from aqueous solution.

Conflict of Interest: The authors declare that there is no conflict of interest.

## ACKNOWLEDGEMENTS

The authors acknowledge the financial support of TETfund Nigeria and the Centre for Research, Innovation and Development, Federal Polytechnic, Ado-Ekiti.

## REFERENCES

[1] Yarkandi N. (2014). Removal of lead (II) from waste water by adsorption. Int. J. Curr. Microbiol. Appl., 3, 207–228.

[2] Nriagu JO. (1989). A global assessment of natural sources of atmospheric trace metals.Nature. 338:47–49.

[3] Abegunde SM, Ogede RO, Fatile BO and Aliu ET (2018). Talinum triangulare leaf andMusa sapientum peel extracts as corrosion inhibitors on ZA-27 alloy. Journal of Particle Science and Technology 4 (1) 23-28

[4] Abegunde SM,, Oyebanji AO and, Osibanjo O. (2018) .Evaluation of Digestion Procedureson Heavy Metals in Soil of a Dumpsite in Ibadan, South-western Nigeria. Suan Sunandha Science and Technology Journal, 5 (2), 1-5.

[5] Kumar A, Kumar A, M M S CP, et al. (2020). Lead Toxicity: Health Hazards, Influence onFood Chain, and Sustainable Remediation Approaches. Int J Environ Res Public Health. 17 (7):2179

[6] Abegunde SM. Akinyele S.A and Awonyemi IO. (2018). Effect of cassava whey on thephysicochemical parameters and heavy metals distribution in soil. Turkish Journal of Agriculture-Food Science and Technology, 6(9), 1196-1199.

[7] Michael AS, Bola DE and Idowu AO. (2018). Assessment of Heavy Metals Distribution andContamination in Atmospheric Dust from Major Roads in Ado-Ekiti, Ekiti State using Pollution Indices International Journal of New Technology and Research, 4(4), 34-40

[8] Abegunde SM, Adejuwon OM and Olorunfemi TO. (2017). Safety Assessment of Hand-DugWell Water Samples from Selected Towns in Ekiti State, Nigeria. Journal of Advanced Research in Applied Chemistry & Chemical Engineering, 4(1&2).40-45

[9] Wani AL, Ara A, Usmani JA. (2015). Lead toxicity: a review. Interdiscip Toxicol. 8(2):55- 64.

[10] Abdulrahman NA and Abegunde SM (2017). Determination Of Selected Heavy Metals in water samples polluted with Municipal wastes around Ibadan North Local Government Area, Ibadan, Oyo State, International Journal Of Current Research In Applied Chemistry & Chemical Engineering, 3 (1) 1-6.

[11] Saravanan R, Sacari E, Gracia F, Khan MM, Mosquera E, GuptaVK. Conducting PANI stimulated ZnO system for visible light photocatalytic degradation of colored dyes. Mol. Liq. J.,

[12] Gupta VK, Jain R, MittalA, Tawfik A, Saleh A, Naya A, Agarwal S, and Sikarwa S. (2012).Photocatalytic degradation of toxic dye amaranth on TiO2/UV in aqueous suspensions. Mater. Sci. Eng. C; 32: 12-17

[13] Saleh TA and Gupta VK. (2012).Photo-catalyzed degradation of hazardous dye methylorange by use of a composite catalyst consisting of multi walled carbon nanotubes and titanium dioxide. J. Colloid Interface Sci. 371: 101-106

[14] Abegunde SM, Idowu KS and Sulaimon AO. (2020), Plant-Mediated Iron Nanoparticles andTheir Applications as Adsorbents for Water Treatment–A Review, Journal of Chemical Reviews, 2(2), 103-113.

[15] Olasehinde EF, Abegunde SM. (2020). Preparation and characterization of a new adsorbent from raphia taedigera seed. Res. Eng. Struct. Mater., 6(2): 167-182.

[16] Bello OS, Adegoke KA, Akinyunni OO. (2017). Preparation and characterization of a noveladsorbent from Moringa oleifera leaf. Appl Water Sci., 7: 1295-1305

[17] Olasehinde, EF, Abegunde, SM. (2020). Adsorption of Methylene Blue onto Acid Modified Raphia taedigera Seed Activated Carbon, Adv. J. Chem. A, 2020, 3(5), 663–679

[18] Mittal A, Mittal J, Malviya A, Kaur D and Gupta VK. (2010). Decoloration treatment of a hazardous triarylmethane dye, light green SF (Yellowish) by waste material adsorbents. J. Colloid Interface Sci., 342: 518-527

[19] Kundu S and Gupta VK, (2006): Arsenic Adsorption onto Iron Oxide-Coated Cement (IOCC): Regression Analysis of Equilibrium Data with Several Isotherm Models and Their Optimization. Chemical Engineering Journal, 122, 93-106.

[20] Foo, KY, (2012). Preparation, characterization and evaluation of adsorptive properties of orange peel based activated carbon via microwave induced K2CO3 activation. Bioresoures Technology, 104: 679–686.

[21] Olasehinde, E.F., Adegunloye, A.V., Adebayo, M.A. and Oshodi, A.A., (2018). Sequestration of Aqueous Lead(II) Using Modified and Unmodified Red Onion Skin, Analytical Letters 51 (17), 2710-2732.

[22] Al-Ghouti, M.A., Khraishe, M.A.M., Allen, S.J. and Ahmad, M.N. (2003). The removal of dyes from textile wastewater: a study of the physical characteristics and adsorption mechanisms of diatomaceous earth. Journal of Environmental Management. 69:229-238.

[23] Xiong, C., Zheng, Y., Feng, Y., Yao, C., Ma, C., Zheng, X. and Jiang, J. (2014). Preparation of a novel chloromethylated polystyrene-2-amino-1,3,4-thiadiazole chelating resin and its adsorption properties and mechanism for separation and srecovery of Pt(IV) from aqueous solutions. Journal of Materials Chemistry A, 2:5379–5386.

[24] Kamaraj, M. and Umamaheswari, P., (2017). Preparation and characterization of Groundnut shell activated carbon as an efficient adsorbent for the removal of Methylene blue dye from aqueous solution with microbiostatic activity. Journal of Materials and Environmental Sciences, 8: 2019 - 2025.

[25] Hameed, B.H., Din, A.T.M. and Ahmad A.L. (2007). Adsorption of methylene blue onto bamboo-based activated carbon: kinetics and equilibrium studies, Journal of Hazardous Materials, 141:819–825.

[26] Sari, A., Tuzen, M., Citak, D. and Soylak, M. (2007). Equilibrium, kinetic and thermodynamic studies of adsorption of Pb(II) from aqueous solution onto Turkish kaolinite clay. Journal of Hazardous Materials, 149:283–91.

[27] Wang, D., Shan, H., Sun, X., Zhang, H. and Wu, Y., (2018). Removal of nitrobenzene from aqueous solution by adsorption onto carbonized sugarcane bagasse. Adsorption Science & Technology, 36:1366–1385.

## AUTHORS

**First Author** – Nurudeen A. Abdulrahman, Department of Science Technology, Federal Polytechnic, Ado-Ekiti, Nigeria
**Second Author** – Akintayo Rotibi, Department of Minerals and Petroleum Resources Engineering Technology, Federal Polytechnic, Ado-Ekiti, Nigeria
**Third Author** – Segun M. Abegunde, Department of Science Technology, Federal Polytechnic, Ado-Ekiti, Nigeria

Correspondence: abegundes@gmail.com